THE JOURNAL OF BIOLOGICAL CHEMISTRY
Vol. 275, No. 24, Issue of June 16, pp. 17954–17961, 2000
© 2000 by The American Society for Biochemistry and Molecular Biology, Inc.
Printed in U.S.A.

Phospholipid Binding of Synthetic Talin Peptides Provides Evidence for an Intrinsic Membrane Anchor of Talin*

Received for publication, March 17, 2000
Published, JBC Papers in Press, March 27, 2000, DOI 10.1074/jbc.M002264200

Anna Seelig‡§, Xiaochun Li Blatter‡, Adrian Frentzel‡, and Gerhard Isenberg¶

From the ‡Department of Biophysical Chemistry, Biocenter, University of Basel, Klingelbergstrasse 70, CH-4056 Basel, Switzerland and the ¶Biophysics Department, Technical University of Munich, D-85747 Garching, Germany

Talin, an actin-binding protein, is assumed to anchor at the membrane via an intrinsic amino acid sequence. Three N-terminal talin fragments, 21–39 (S19), 287–304 (H18), and 385–406 (H17) have been proposed as potential membrane anchors. The interaction of the corresponding synthetic peptides with lipid model systems was investigated with CD spectroscopy, isothermal titration calorimetry, and monolayer expansion measurements. The membrane model systems were neutral or negatively charged small unilamellar vesicles or monolayers with a lateral packing density of bilayers (32 mN/m). S19 partitions into charged monolayers/bilayers with a penetration area A_p = 140 ± 30 Å^2 and a free energy of binding of $\Delta G_0 = -5.7$ kcal/mol, thereby forming a partially α-helical structure. H18 does not interact with lipid monolayers or bilayers. H17 penetrates into neutral and charged monolayers/bilayers with A_p = 148 ± 23 Å^2 and A_p = 160 ± 15 Å^2, respectively, forming an α-helix in the membrane-bound state. Membrane partitioning is mainly entropy-driven. Under physiological conditions the free energy of binding to negatively charged membranes is $\Delta G_0 = -9.4$ kcal/mol with a hydrophobic contribution of $\Delta G_h = -7.8$ kcal/mol, comparable to that of post-translationally attached membrane anchors, and an electrostatic contribution of $\Delta G_h = -1.6$ kcal/mol. The latter becomes more negative with decreasing pH. We show that H17 provides the binding energy required for a membrane anchor.

Talin is a widespread actin-binding protein present in focal cell adhesions and ruffling membranes of moving cells (1, 2). In fibroblasts, talin binding to lipid membranes is associated with the establishment of a signaling cascade, mediated either by integrins (3, 4) leading to the formation of focal adhesions or, alternatively, by layilin (5) leading to a nucleation of actin assembly in membrane ruffles. In platelets, talin redistributes from the cytoplasm to the membrane during activation (6) where it colocalizes with the GPIIb/IIIa complex (7). Talin analogues have been identified in lower organisms like *Dictyostelium* (8) and *Caenorhabditis elegans* (9), the N termini and C termini being most preserved.

Reasons to assume that talin is involved in a polarized assembly of the actin cytoskeleton by nucleating actin filament growth at lipid interfaces (10, 11) were provided from the finding that *Dictyostelium* mutants, which lack the entire protein, are massively impaired in adhesion and motility (12), and HeLa cells, when down-regulated in talin expression by antisense RNA, exhibit a reduced rate in cell spreading (13). Antibodies directed against talin, when microinjected were shown to inhibit fibroblast migration (14).

Some of talin's functions have been attributed to specific protein domains. Calpain or thrombin cleavage *in vitro* yields two parts with 190 and 47 kDa, respectively. The C-terminal 190-kDa portion was shown to carry the actin binding sites (15) in form of a conserved sequence, the (I/L)WEQ module (16), and to be responsible for actin nucleation (17) and cross-linking (18, 19). The membrane binding capacity of talin exclusively resides in the 47-kDa N-terminal portion (20). Binding of the entire talin molecule to negatively charged phospholipid bilayers has been measured, resulting in an overall binding constant of $K = 2.9 \cdot 10^6$ M^{-1} (21).

Unraveling the talin-lipid membrane interaction on a molecular level is a prerequisite for understanding the redistribution of talin from the cytoplasm to the membrane surface upon cell activation as a principal step in the initiation of a signal transduction cascade. Unlike hisactophilin, an actin-binding protein that interacts with membranes by means of a post-translationally attached myristoyl anchor (22), talin is supposed to bind to phospholipid membranes via an interaction of intrinsic amino acid sequences. A similar mechanism was also proposed for vinculin (23, 24).

On the basis of secondary structure predictions, three small segments of the 47-kDa head portion of the talin homodimer, corresponding to amino acid residues 21–39 (S19), 287–304 (H18), and 385–406 (H17), were suggested to be responsible for lipid binding (23, 25).

The aim of the present investigation is to experimentally test the membrane binding potential of the three talin peptides and to discuss their role as likely membrane anchors of talin. To this purpose the respective peptides have been synthesized. As membrane model systems, we chose electrically neutral or negatively charged small unilamellar vesicles (SUVs)[1] and lipid monolayers at a packing density corresponding to that of a lipid bilayer (32 mN/m) (26). The lipid model systems were composed of either 1-palmitoyl-2-oleoyl-*sn*-3-phosphatidylcholine (POPC) or of a mixture of POPC and 1-palmitoyl-2-oleoyl-*sn*-3-phosphatidylglycerol (POPG) in a molar ratio (3/1), mimicking the negative surface potential of the lipid leaflet facing the cytoplasm. The peptide conformations in solution and when bound to neutral and negatively charged SUVs are analyzed by means of CD spectroscopy. Their partition coefficients are measured using high sensitivity isothermal titration calorimetry and

* This work was supported by Swiss National Science Foundation Grant 31.42058.94 and by Sonderforschungsbereich Grant 266/C-5 (to G. I.). The costs of publication of this article were defrayed in part by the payment of page charges. This article must therefore be hereby marked "*advertisement*" in accordance with 18 U.S.C. Section 1734 solely to indicate this fact.

§ To whom correspondence should be addressed. Fax: 41-61-267-21-89; E-mail: anna.seelig@unibas.ch.

[1] The abbreviations used are: SUV, small unilamellar vesicle; POPC, 1-palmitoyl-2-oleoyl-*sn*-3-phosphatidylcholine; POPG, 1-palmitoyl-2-oleoyl-*sn*-3-phosphatidylglycerol; deg, degrees; N, newton(s).

This paper is available on line at http://www.jbc.org

Downloaded from http://www.jbc.org/ at Universitaetsbibliothek Medizin on November 20, 2017

TABLE I
Amino acid sequence of talin peptides

Residues	Name	Sequence
		+ − + +−+ −
21–39	(S19)	PSTMVYDACRMIRERIPEA-$CONH_2$
		+ − − + + + +
287–304	(H18)	GQMSEIEAKVRYVKLARS-$CONH_2$
		+− − ++++ +
385–406	(H17)	GEQIAQLIAGYIDIILKKKKSK-$CONH_2$

monolayer expansion measurements at different ionic strength and pH values. A comparison of the partition coefficients of talin peptides with those of a myristoyl or a farnesyl anchor suggests that H17 could indeed function as the principal intrinsic membrane anchor of talin.

MATERIALS AND METHODS

Talin Peptides—The three fragments from mouse talin (27) were synthesized by BioGenes, Berlin, Germany as trifluoro-acetate (S19 and H18) and chloride salts (H17), as shown in Table I. Purity as determined by high pressure liquid chromatography was >90% for S19 and H18 and >96% for H17. The peptide contents were determined by quantitative amino acid analysis.

Buffers—All buffers used were adjusted to pH 7.4 at the temperatures used for the respective measurements. For monolayer expansion measurements (T = 23 ± 1 °C), 50 mM Tris/HCl buffer containing 114 mM NaCl was used. For circular dichroism (CD) spectroscopy (T = 23 ± 1 °C), 10 mM Tris/HCl buffer, with or without 154 mM NaF, was prepared. NaF was used instead of NaCl, since the latter strongly absorbs at low wavelength. For isothermal titration calorimetry (T = 28 °C), 50 mM Tris/HCl buffer with or without 114 mM NaCl was used.

Lipid Vesicle Preparation—POPC and POPG were purchased from Avanti Polar Lipids (Birmingham, AL) and were used without further purification. Small unilamellar vesicles of ~30 nm diameter were prepared for CD spectroscopy and isothermal titration calorimetry as follows; POPC and POPG were dissolved in chloroform (~20 mg/ml) in appropriate molar ratio. The solvent was first evaporated under a nitrogen stream leading to a thin lipid film. To improve the homogeneity of the lipid mixture, the film was redissolved in dichloromethane, dried again under nitrogen, and subsequently dried under high vacuum overnight. The amount of lipid was determined gravimetrically, and buffer was added to the dry lipid film to the desired concentration. The lipid dispersion was vortexed and then sonicated under a nitrogen atmosphere at 5 °C until an almost clear solution was obtained. For negatively charged lipids sonification time was ~20 min, and for electrically neutral lipids ~35 min. Metal debris from the titanium tip was removed by centrifugation in an Eppendorf centrifuge at 14,000 rpm for 8 min.

Circular Dichroism Measurements—Circular dichroism (CD) spectra were measured with a Jasco J720 spectropolarimeter at ambient temperature. The path length of the cell was 1 mm. Spectra of peptides in solution were corrected by subtracting the buffer base line. Spectra of peptides in the presence of lipid vesicles were corrected by subtracting the spectra of the corresponding lipid vesicle dispersions.

The fraction of β-sheet structure in solution was estimated by means of computer simulations based on the reference spectra of Yang *et al.* (28) as well as on the basis of the spectra of Greenfield and Fasman (29).

The α-helical fraction, f_h, was determined according to Chen et al. (30).

$$f_h = \frac{[\theta]_{222}}{\theta_h^n} \quad \text{(Eq. 1)}$$

[Θ] is the mean residue ellipticity, in units of degrees (deg) cm^2 dmol^{-1} measured at 222 nm and Θ_h^n is the maximum absorptioon of an α-helix with n amino acid residues and is determined as follows.

$$\theta_h^n = (1 - k/n)\theta_h^\infty \quad \text{(Eq. 2)}$$

k is a wavelength-dependent constant (k_{222} = 2.57) and Θ_h^∞ is the maximum ellipticity of an α-helix with infinite length (Θ_h^∞ = −39,500 deg cm^2 dmol^{-1}).

Monolayer Expansion Measurements—The monolayer apparatus designed by Fromherz (31) consists of a round Teflon trough with a total area of 362 cm^2, divided into eight compartments (type RCM 2-T, Mayer Feintechnik, Göttingen, Germany). For lipid monolayer expansion experiments, two compartments were used, containing together 40 ml of solution. In order to keep humidity constant, the trough was covered by a Plexiglas hood, and compartments that were not used for measurements were filled with water. The surface pressure, $\pi = \gamma_0 - \gamma$, where γ_0 is the surface tension of the pure buffer and γ the surface tension of the peptide solution, was monitored by means of a Whatman no. 1 filter paper, connected to a Wilhelmy balance.

The monolayer was formed by depositing a drop of lipid dissolved in hexane/ethanol (9/1, v/v) on the buffer surface between a fixed and a movable barrier, and was then left to stabilize for about 15 min. The initial area, A, of the lipid monolayer was typically around 50 cm^2 and contained n_L lipid molecules. Peptide dissolved in pure water (~0.1 mM) was injected with a Hamilton syringe into the buffer subphase, which was stirred continuously by a magnetic stirring bar. During equilibration time (~40–50 min), the surface pressure π was kept constant by means of an electronic feedback system.

The penetration of n_P peptide molecules into the monolayer with a penetration area, A_P, gives rise to an area expansion ΔA.

Evaluation of the Partition Coefficient from Monolayer Expansion Measurements—The mole fraction of peptide in the monolayer is defined as $X_b = n_P/n_L$, and can be evaluated from the relative area increase, $\Delta A/A$, provided A_L and A_P (*cf.* next paragraph) are known (26).

$$X_b = n_P/n_L = (\Delta A/A)\,(A_L/A_P) \quad \text{(Eq. 3)}$$

The apparent partition coefficient, K_{app}, is

$$K_{app} = (\Delta A/A)\,(A_L/A_P)/C_{eq} = X_b/C_{eq} \quad \text{(Eq. 4)}$$

The equilibrium peptide concentration, C_{eq}, is the difference between the total peptide concentration, C_0, and the concentration of the bound peptide, C_b.

$$C_{eq} = C_0 - C_b \quad \text{(Eq. 5)}$$

Measurement of the Penetration Area of Peptides—In order to penetrate into a lipid monolayer with a lateral pressure, π, a peptide molecule has to perform the work $\Delta W = \pi A_p$, where the penetration area, A_p, is the cross-sectional area of the peptide portion in the lipid monolayer. The free energy of penetration will vary with the monolayer surface pressure π. According to Ref. 32, the variation of the partition coefficient, K_{app}, with the surface pressure is given by the following equation.

$$K_{app} = K_0 e^{-\pi A_P/kT} \quad \text{(Eq. 6)}$$

K_0 is a proportionality constant. Combining Equations 4 and 6 yields the surface pressure dependence of the relative area increase, $\Delta A/A$, at constant C_{eq} under the assumption of a constant penetration area, A_p, and a constant lipid area, A_L.

$$\Delta A/A = (A_p/A_L)K_0 C_{eq} e^{-\pi A_P/kT} \approx \text{const.} e^{-\pi A_P/kT} \quad \text{(Eq. 7)}$$

The assumption of constant areas can be made to a first approximation since A_L and A_p change by at most 15% in the given surface pressure interval. According to Equation 7, the penetration area, A_p, is determined from the slope of the ln $\Delta A/A$ *versus* π curve.

Analysis of Binding Isotherm by Means of the Gouy-Chapman Theory—Partitioning of cationic peptides into an electrically neutral lipid/water interface gives rise to a positive surface potential, ψ_0, of the lipid layer. As a consequence the concentration of the cationic peptide at the membrane surface, C_M, decreases ($C_{eq} > C_M$). Negatively charged lipid monolayers exhibit, in contrast, a negative surface potential that leads to an accumulation of cationic peptides close to the membrane surface ($C_{eq} < C_M$). The relationship between the membrane-active concentration, C_M, and the bulk concentration, C_{eq}, is given by the Bolzmann equation.

$$C_M = C_{eq} e^{-\psi_0 z_{eff} F_0/RT} \quad \text{(Eq. 8)}$$

The surface potential, ψ_0, can be approximated by means of the Gouy-Chapman theory (for details, *cf.* Ref. 33). The peptide charge is denoted as z_{eff}. The surface partition equilibrium can then be formulated as shown by Equation 9.

$$K_p = X_b/C_M \quad \text{(Eq. 9)}$$

K_p is the hydrophobic partition coefficient. The Gouy-Chapman theory thus allows a separation of hydrophobic (K_p) and electrostatic (z_{eff}) contributions to membrane binding.

High Sensitivity Titration Calorimetry—Isothermal titration calo-

Downloaded from http://www.jbc.org/ at Universitaetsbibliothek Medizin on November 20, 2017

rimetry was performed using an Omega high sensitivity titration calorimeter from MicroCal (Northampton, MA) (34). To avoid air bubbles, solutions were degassed under vacuum before use. The calorimeter was calibrated electrically. The data were acquired using computer software developed by MicroCal. In control experiments the corresponding suspension of SUVs (or peptide solution) was injected into buffer without peptide (lipid). Both experiments yielded small reaction heats, which were included in the final analysis.

Evaluation of Partition Coefficients from High Sensitivity Titration Calorimetry—SUVs are injected into a peptide solution, causing peptide molecules to partition into the lipid bilayer. The reaction enthalpy measured at the ith lipid injection is denoted as Δh_i, and the cumulative heat of reaction after the first k injection steps is $\Sigma_{i=1}^{k}\Delta h_i$. The molar amount of bound peptide, $n_p^{(k)}$, is then given by Equation 10.

$$n_p^{(k)} = \sum_{i=1}^{k}\Delta h_i/\Delta H \qquad \text{(Eq. 10)}$$

ΔH is the molar reaction enthalpy. The total amount of injected lipid, $n_L^{(i)}$, is given by Equation 11.

$$n_L^{(k)} = C_L^0 \cdot V_{inj} \cdot k \qquad \text{(Eq. 11)}$$

C_L^0 is the lipid concentration of the stock solution, V_{inj} the volume per injection, and k the number of injections. Under the present experimental conditions, the binding of peptides is presumably limited to the outside of the lipid vesicles (35). For sonified lipid vesicles with a diameter of 30 nm, about 60% of the total lipid resides on the outside. The mole fraction of bound peptide in the lipid layer, $X_b^{(k)}$, is hence given by Equation 12.

$$X_b^{(k)} = n_p^{(k)}/(0.6 \cdot n_L^{(k)}) \qquad \text{(Eq. 12)}$$

The correction factor 0.6 accounts for the lipid molecules on the vesicle outer layer. Knowledge of the bound peptide allows the calculation of the remaining free peptide concentration, C_{eq}. A plot of $X_b^{(k)}$ *versus* C_{eq} yields the binding isotherm. From the binding isotherms the apparent partition coefficient, K_{app}, can be calculated according to Equation 4.

$$K_{app} = X_b^{(k)}/C_{eq} \qquad \text{(Eq. 13)}$$

RESULTS

The Secondary Structure of Talin Peptides in Solution—The conformations of the three talin peptides were investigated by means of CD spectroscopy in buffer solution at pH 7.4 and at physiological salt concentrations (10 mM Tris/HCl, 154 mM NaF). All three peptides show a minimum around 200 nm with a mean residue ellipticity, $[\Theta]_{200} \leq -10{\cdot}10^3$ deg cm^2 dmol^{-1} and a broad shoulder around 217 nm, suggesting a mixture of random coil and β-sheet conformations, increasing in the order H18 < S19 < H17.

For H17 (10 μM), the β-sheet content is estimated as ~30% according to Greenfield and Fasman (29) in good agreement with computer simulations using the method of Yang *et al.* (28). The concentration of monomers in solution, C_A, is evaluated according to (36).

$$C_A = C_0(1 - X_\beta) \qquad \text{(Eq. 14)}$$

C_0 is the total peptide concentration, and X_β is the mole fraction of monomers involved in β-sheet formation and can be calculated as shown in Equation 15.

$$X_\beta = (\%\ \beta \text{ observed})/(\text{maximum } \%\ \beta\text{-structure}) \qquad \text{(Eq. 15)}$$

The maximum amount of β-sheet structure for H17 is 63%, assuming that the charged ends (8 residues) are fraying. With a β-structure content of 30%, the monomer concentration is determined as C_A = 5.0 μM, which corresponds to 50% of the total peptide concentration.

Despite the tendency to self-associate, the three peptides are highly soluble in aqueous solution and yield clear solutions even at millimolar concentrations.

The Secondary Structure of Talin Peptides in the Presence of Lipid Vesicles—The titrations of the three talin peptides with POPC/POPG (3/1) and POPC vesicles in buffer solution at pH 7.4 and different salt concentrations are summarized in Fig. 1. The mean residue ellipticity, $[\Theta]_{222}$ at 222 nm, which is a measure for the extent of α-helix formation, is plotted as a function of the lipid-to-peptide molar ratio. The tendency to form α-helical structures upon binding to POPC/POPG (3/1) vesicles in buffer solution (pH 7.4, 10 mM Tris/HCl) increases in the order of H18 ≪ S19 < H17 in the presence (154 mM NaF) as well as in the absence of salts (not shown for H18 and S19). Binding to POPC vesicles is only observed for H17.

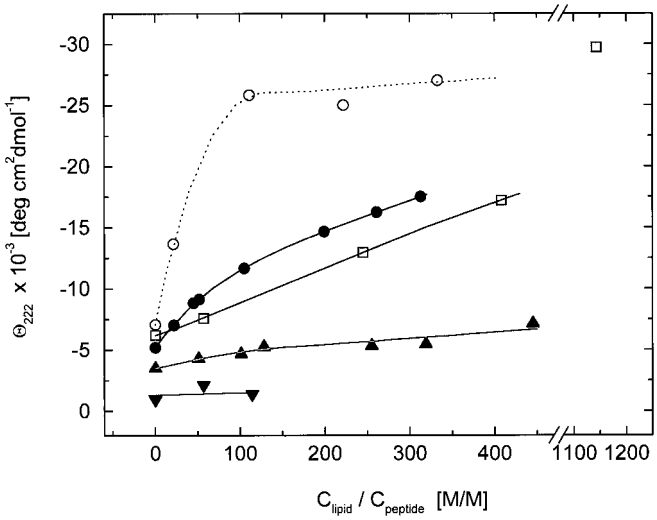

FIG. 1. **Mean residue ellipticity $[\Theta]_{222}$ measured as a function of the lipid-to-peptide ratio in 10 mM Tris/HCl buffer at pH 7.4 with 154 mM (*solid symbols*) and without NaF (*open symbols*).** Figure shows H18 ($C_0 = 3.7{\cdot}10^{-5}$) (▼) M, S19 ($C_0 = 4.9{\cdot}10^{-5}$) (▲), and H17 ($C_0 = 1.5{\cdot}10^{-5}$) (●, ○) in the presence of SUVs formed by POPC/POPG (3/1 molar ratio); H17 ($C_0 = 1.0{\cdot}10^{-5}$) (□) in the presence of SUVs formed by POPC.

In the absence of salts (pH 7.4, 10 mM Tris/HCl), the degree of H17 α-helicity induced by POPC/POPG (3/1) as well as by POPC vesicles reaches a final value of ~86%. Despite this high degree of helicity, CD measurements are not suited for the quantitative evaluation of binding isotherms since H17 induces vesicle fusion at low lipid-to-peptide ratios, especially in the presence, but also in the absence, of salts,[2,3] which leads to light scattering and optical flattening effects (37).

Gibbs Adsorption Isotherms—Fig. 2 shows the surface pressure, π, as a function of concentration, C (Gibbs adsorption isotherms), of the three talin peptides. At a given concentration the surface activity of the peptides increases in the order H18 < S19 < H17. H18 shows a surface pressure onset at $C = 1{\cdot}10^{-7}$ M followed by an almost linear increase of the surface pressure, π, with log C, which is typical for a peptide in a random coil conformation (38). Around $C = 8.5{\cdot}10^{-6}$ M, a steplike increase in surface pressure, π, with concentration, C, is observed, which indicates a pK_a shift due to peptide association (39). For S19 and H17, a surface pressure onset is observed at $C = 1.2{\cdot}10^{-8}$ and $C = 4{\cdot}10^{-9}$ M, respectively, followed by a steep sigmoidal surface pressure increase. At $C = 1.6{\cdot}10^{-6}$ M (S19) and $C = 1{\cdot}10^{-6}$ M and $C = 2{\cdot}10^{-6}$ M (H17), a step-like increase in surface pressure, π, with concentration, C, is observed, again indicating a pK_a shift due to peptide association.

For comparison, the concentrations of surface activity onset of the peptide hormones, substance P (39) and somatostatin (33) is in the order of $C \sim 10^{-6}$ M and the maximum surface

[2] S. Doerhoefer and G. Isenberg, unpublished results.
[3] X. Li Blatter and A. Seelig, unpublished results.

Downloaded from http://www.jbc.org/ at Universitaetsbibliothek Medizin on November 20, 2017

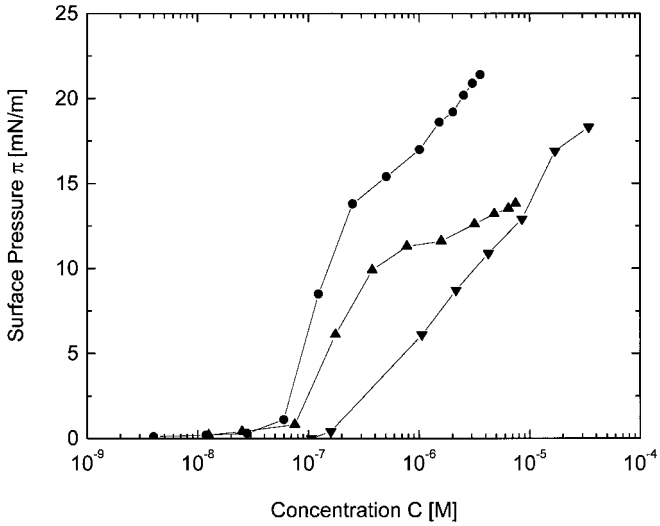

FIG. 2. **Surface pressure, π, as a function of concentration (Gibbs adsorption isotherm) for H18 (▼), S19 (▲), and H17 (●) at pH 7.4 (50 mM Tris, 114 mM NaCl).**

activity reached is lower. The Gibbs adsorption isotherm thus provides direct evidence for the strong hydrophobicity and amphiphilicity of the present peptides.

Peptide Penetration Areas—A lipid monolayer with a given initial area, A, and a surface pressure, π, kept constant during the insertion measurement, was spread on a buffer surface (pH 7.4, 50 mM Tris/HCl, 154 mM NaCl). Injection of the peptide into the buffer subphase gave rise to an area increase, ΔA, due to the insertion of peptides into the lipid layer. The area increase, ΔA, of a POPC/POPG (3/1) monolayer due to insertion of H17 as a function of time is shown in Fig. 3*A*. The equilibration time was 30–50 min. Fig. 3*B* shows the relative area increase, $\Delta A/A$, upon penetration of H17 into POPC/POPG (3/1) and POPC monolayers as a function of the surface pressure, π. The concentrations of H17 used were $C_0 = 1.6 \cdot 10^{-7}$ and $C_0 = 5.7 \cdot 10^{-7}$ M, respectively. Each measurement was performed with a new lipid monolayer with a preset surface pressure, π. H17 inserts into neutral and negatively charged monolayers in the whole surface pressure range measured ($\pi \cong 24$–32 mN/m). In the same surface pressure range, S19 ($C_0 = 4.2 \cdot 10^{-6}$ M) inserts only into negatively charged monolayers (data not shown). H18 does not penetrate into lipid monolayers, not even at low surface pressures and relatively high concentrations ($\sim 10^{-5}$ M).

From the slope of the ln $\Delta A/A$ *versus* π curves (Equation 7), the penetration area of S19 and H17 in POPC/POPG (3/1) monolayers is estimated as $A_p = 140 \pm 30$ Å^2 and $A_p = 160 \pm 15$ Å^2, respectively, and that of H17 in POPC monolayers as $A_p = 148 \pm 23$ Å^2.

Binding Isotherms Measured by Means of the Monolayer Expansion Technique—The partitioning of peptides S19 and H17 into lipid monolayers was measured by monitoring the relative area increase, $\Delta A/A$, as a function of the equilibrium concentration, C_{eq}, at constant surface pressure, π. The surface pressure was $\pi = 32$ mN/m, corresponding to the lateral packing density of a POPC bilayer (26). The relative area increase, $\Delta A/A$, was transformed into the mole fraction of bound peptide, X_b, according to Equation 4 using the penetration area, A_P, of the peptides and the area, $A_L = 65$ Å^2 per lipid molecule.[4] Fig. 3*C* shows the binding isotherm of H17 for POPC/POPG (3/1) monolayers at 32 mN/m. The *solid line* corresponds to a binding isotherm calculated on the basis of the Gouy-Chapman theory using a charge $z = +0.9$, a p$K_a = 7.6$ for the N-terminal amino group, and a hydrophobic partition coefficient, $K_p = 8.5 \cdot 10^3$ M^{-1}. The pH of the solution and the binding constant of sodium ions ($K_0 = 0.6$ M^{-1}) are taken into account (33).

The apparent partition coefficient of H17 for POPC monolayers was calculated as $K_{app} = (1.2 \pm 0.3) \cdot 10^4$ M^{-1} in good agreement with the hydrophobic partition coefficient, K_p, determined by means of the Gouy-Chapman theory for negatively charged monolayers. The apparent partition coefficient of H17 for POPC/POPG (3/1) monolayers (comprising electrostatic and hydrophobic contributions) was $K_{app} = (1.1 \pm 0.2) \cdot 10^5$ M^{-1}. The apparent partition coefficient of S19 for POPC/POPG (3/1) monolayers was $K_{app} = (2.4 \pm 0.8) \cdot 10^2$ M^{-1}.

Binding Isotherms Measured by Means of High Sensitivity Titration Calorimetry—The thermodynamics of the partitioning of the three talin peptides into POPC and POPC/POPG (3/1) small unilamellar vesicles was investigated by means of high sensitivity isothermal titration calorimetry (for review, see Ref. 35). Experiments were performed at pH 7.4 (50 mM Tris/HCl) with and without 114 mM NaCl. Aliquots (10 μl) of a suspension of sonified POPC or POPC/POPG (3/1) (25–35 mM) vesicles were injected into the calorimeter cell ($V_{cell} = 1.3343$ ml) containing the peptide solution. For S19 and H18 the initial peptide concentration used was $C_0 = 22.9$ μM. For H18 no binding reaction could be measured. For S19 the apparent partition coefficient for POPC/POPG (3/1) vesicles was determined as $K_{app} = (4.0 \pm 1) \cdot 10^2$ M^{-1}, in broad agreement with that determined by means of the monolayer expansion technique. For POPC vesicles the partition coefficient was too small to be measured.

For H17 titrations were performed in four different concentration intervals. The highest concentrations of the respective intervals were $C_0 = 10$, 7.8, 5, and 2.5 μM. Each injection gave rise to an exothermic heat of reaction, h_i, produced by the peptide partitioning into the lipid membrane. As an example the titration of H17 with POPC/POPG (3/1) vesicles is shown in Fig. 4*A*. The heat of reaction decreases with consecutive injections, because after each injection less free peptide is available for binding. As a control the same lipid vesicle suspension was injected into buffer without peptide. The heat of dilution, h_c, was small and constant during consecutive injections. The quantitative analysis of the data was based on the corrected heats of titration, Δh_i, given by Equation 16.

$$\Delta h_i = h_i - h_c \qquad \text{(Eq. 16)}$$

The cumulative heat of reaction after k injections, ΔH_k, is defined as shown in Equation 17, and is shown in Fig. 4*B*.

$$\Delta H_k = \sum_{i=1}^{k} \Delta h_i \qquad \text{(Eq. 17)}$$

The average molar reaction enthalpy of H17 for binding to POPC vesicles was $\Delta H = -5.6$ kcal/mol and that for binding to POPC/POPG (3/1) vesicles was $\Delta H = -2.5$ kcal/mol.

Binding isotherms were also measured at pH 6.0. Under these conditions binding increased and strong aggregation occurred that hampered a quantitative analysis of the data.

The apparent partition coefficients, K_{app}, of H17 measured for lipid monolayers at 32 mN/m and for small unilamellar vesicles under different conditions are summarized in Fig. 5. At the lowest concentrations measured, the apparent partition coefficients for neutral POPC and negatively charged POPC/POPG (3/1) membrane model systems differ by a factor of ~10. With increasing concentration, the difference between the par-

[4] We assume that the average area per lipid molecule in a POPC/POPG (3/1) monolayer is identical to that in a POPC monolayer (52) to a first approximation.

Downloaded from http://www.jbc.org/ at Universitaetsbibliothek Medizin on November 20, 2017

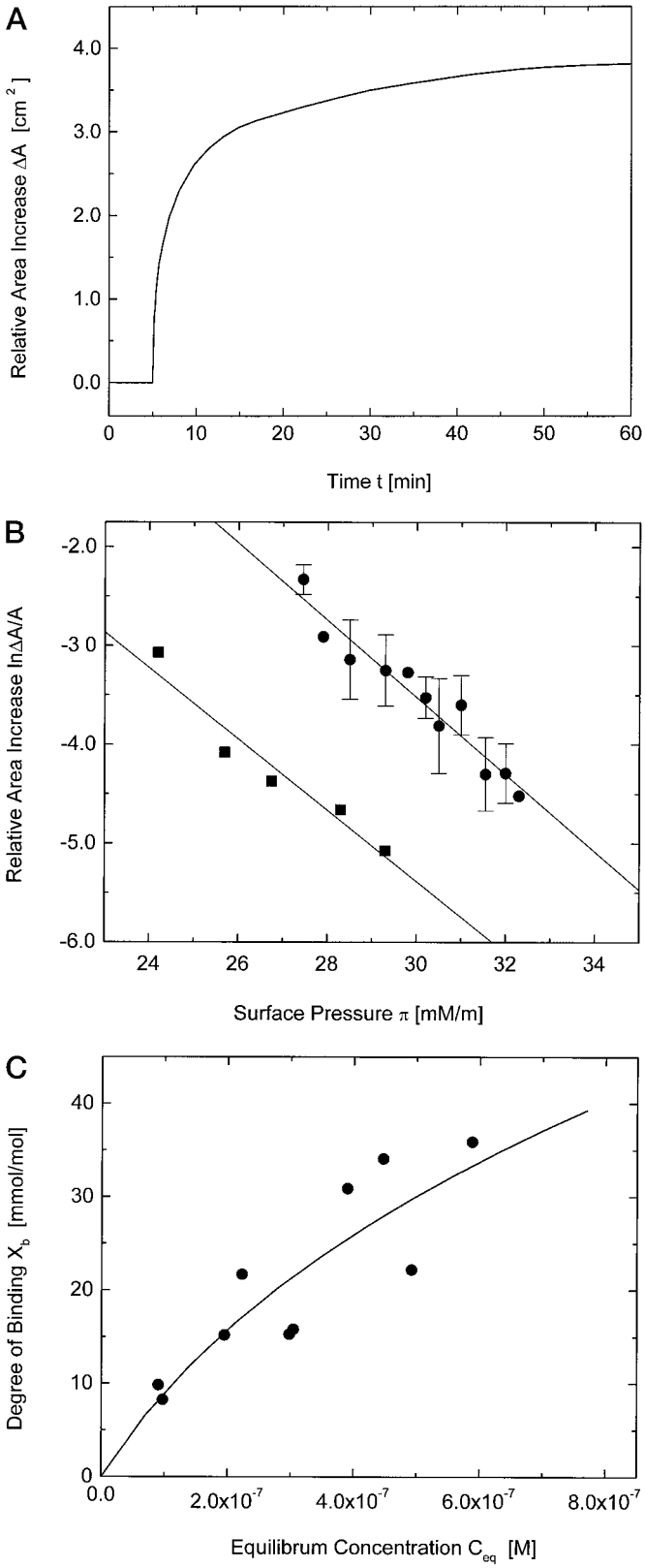

FIG. 3. *A*, the area increase, ΔA, upon penetration of H17 (C_{eq} = $4.49 \cdot 10^{-7}$) into a POPC/POPG (3/1 molar ratio) monolayer at a constant surface pressure (32 mN/m) is plotted as a function of time (pH 7.4 (50 mM Tris/HCl, containing 114 mM NaCl). *B*, relative area increase, ln $\Delta A/A$, as function of the surface pressure, π, due to the penetration of H17 into POPC/POPG (3/1 molar ratio) (●) and POPC monolayers (■). Peptide concentrations are $C_0 = 1.6 \cdot 10^{-7}$ M and $C_0 = 5.7 \cdot 10^{-7}$. Each measurement was made with a new lipid monolayer kept at a constant surface pressure, π. *Symbols* without *error bars* represent single measurements. *Symbols* with *error bars* represent the mean values of two or three independent measurements. *C*, binding isotherm of H17 in the presence of POPC/POPG (3/1 molar ratio) monolayers at 32 mN/m in buffer solution (pH 7.4, 50 mM Tris/HCl, containing 114 mM NaCl). Each point is an independent measurement with a new lipid monolayer. The *solid line* represents the theoretical binding isotherm calculated by means of the Gouy-Chapman theory using a charge, $z = +0.9$ for the lysine residues, a $pK_a = 7.6$ for the N-terminal amino group (total effective charge $z_{eff} = +1.7$), and a hydrophobic partition coefficient, $K_p = 8.5 \cdot 10^3$; the pH and the salt concentration are taken into account.

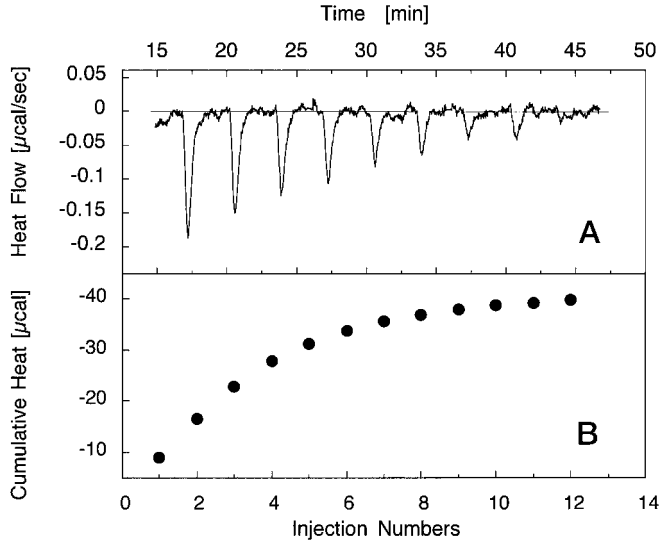

FIG. 4. *A* and *B*, isothermal titration calorimetry of H17 (C_{pep} = 7.8 μM) with small unilamellar POPC/POPG (3/1 molar ratio) vesicles (C_{lip} = 25 mM) at pH 7.4 (50 mM Tris/HCl, 114 mM NaCl) at 28 °C. Each peak corresponds to the injection of 10 μl of stock solution into the calorimeter cell. *A*, calorimeter tracing; *B*, cumulative heat, $\Sigma_{i=1}^{k} \Delta h_i$, calculated from the area underneath the titration peaks, as a function of the number of injections. The heat of dilution (small endothermic reactions), measured in separate control experiment, was subtracted in *A* and *B*.

tition coefficients for neutral and negatively charged bilayer model systems decreases (*cf.* "Discussion"). The apparent partition coefficients measured in the absence of salts are similar to those measured in the presence of salts.

DISCUSSION

In vivo, talin is found in equilibrium between a membrane-bound and a cytosolic form as observed for other actin-binding proteins (*e.g.* hisactophilin (Ref. 22)). The lipids of the cytoplasmic side of the membrane could provide a matrix for talin anchorage and for two-dimensional diffusion to its effector sites, *e.g.* the membrane spanning proteins, integrin and/or layilin. The three N-terminal talin fragments S19 (residues 21–39), H18 (residues 287–304), and H17 (residues 385–406) have been suggested to act as potential membrane anchors (23, 25). Peptides corresponding to these fragments were therefore synthesized, and their binding to lipid bilayers and to monolayers at a lateral packing density corresponding to that of lipid bilayers (26) was measured. The membrane model systems were either composed of electrically neutral POPC or of a mixture of POPC/POPG in a molar ratio (3/1) mimicking the negative surface charge density of the cytoplasmic membrane leaflet. We will first analyze the binding data, which are nontrivial due to the strong hydrophobicity and amphiphilicity of the peptides, and second, we will discuss the suitability of the peptides as potential membrane anchors. It will be shown that the hydrophobic binding energy of H17 is comparable to that of post-translationally attached membrane anchors.

Membrane Penetration and Helix Formation Correlates with

Downloaded from http://www.jbc.org/ at Universitaetsbibliothek Medizin on November 20, 2017

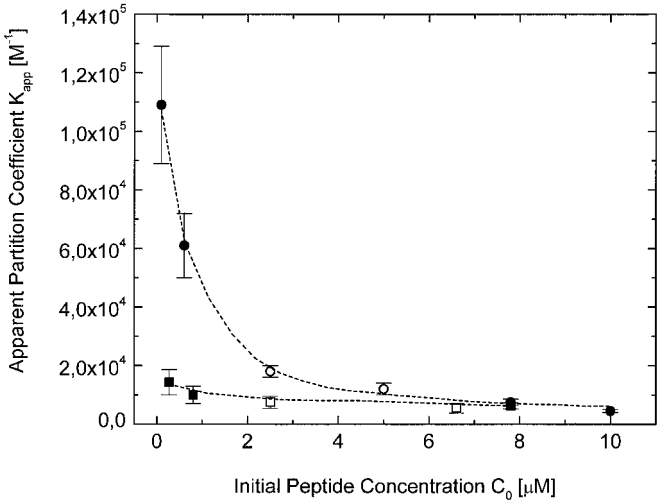

FIG. 5. **The apparent partition coefficients, K_{app}, of H17 measured in different concentration intervals are shown as a function of the concentration, C_0, corresponding to the total peptide concentration at the upper boundary of the respective intervals.** The partition coefficient for the lowest concentration interval was determined by means of the monolayer expansion technique at 32 mN/m; the other partition coefficients were measured by means of isothermal titration calorimetry. Lipid model systems are composed of POPC (■, □) and or POPC/POPG (3/1 molar ratio) (●, ○). Measurements were performed in buffer at pH 7.4 (50 mM Tris/HCl) with 114 mM NaCl (*solid symbols*) and without NaCl (*open symbols*).

the Amphipathic Nature of the Peptides—The helical wheel projections (40) of the three talin peptides are displayed in Fig. 6 (*A–C*). S19 shows some amphipathic character (Fig. 6*A*); however, the three cationic residues are not concentrated on one side of the helix. H18 is even less amphipathic (Fig. 6*B*). H17 forms, in contrast, a five-loop α-helix, where the four N-terminal loops are strongly amphipathic with a hydrophilic surface and a larger hydrophobic surface comprising five isoleucines. The C-terminal loop consists of the sequence K-K-K-K-S-K (Fig. 6*C*).

S19 penetrates into POPC/POPG (3/1) monolayers at micromolar concentrations with a penetration area, $A_p = 140 \pm 30$ Å^2 in the whole surface pressure range measured (24–32 mN/m) and concomitantly forms a partially α-helical structure.

H18 does not insert into POPC/POPG (3/1) monolayers in the surface pressure range of 24–32 mN/m, not even at relatively high concentrations ($C_0 \sim 10^{-5}$ M). Neither does it form secondary structures in the presence of POPC/POPG (3/1) and POPC vesicles.

H17 penetrates into POPC/POPG (1/3) *and* POPC monolayers at submicromolar concentrations with penetration areas, $A_p = 160 \pm 15$ Å^2 and $A_p = 148 \pm 23$ Å^2, respectively, in the whole surface pressure range measured (24–32 mN/m) and concomitantly forms α-helical structures. The maximum helicity observed was ~86% in both systems. This high degree of α-helicity could, however, only be observed in the absence of salts. The main reason for the apparently lower α-helicity in the presence of physiological salt concentrations is due to vesicle fusion and concomitant light scattering and optical flattening (37) effects, which are more pronounced in the presence than in the absence of salts.[3] Considering the fact that the apparent binding constants were almost independent of the salt concentrations (*cf.* Fig. 5), a reduction of the α-helicity as a result of charge screening effects can be excluded.

The measured penetration area of H17 is too small to assume a deep insertion of the entire hydrophobic surface of the molecule oriented parallel to the membrane surface. It suggests either a peripheral insertion of the α-helix oriented parallel to the membrane surface or an insertion of the helix oriented more or less parallel to the long molecular axis of the lipids. Considering the hydrophobicity of H17, the latter possibility seems more probable.

The amphipathic character of these peptides is thus directly correlated with their tendency to penetrate into lipid monolayers/membranes and to concomitantly form α-helical structures in the presence of lipid vesicles.

The Apparent Partition Coefficient Is Concentration-dependent Due to Peptide Self-association in Solution—Peptides are assumed to partition into the membrane in their monomeric form. Self-association in solution thus reduces peptide partitioning into the membrane (41). This factor is often neglected. To address this problem, which is especially relevant for H17, we investigated a larger concentration range than generally used for binding studies ($C_0 \sim 0.1$–10 μM). This range was subdivided into seven intervals, for which the partition coefficients were determined (Fig. 5). At the lowest concentrations the partition coefficients were determined using the monolayer expansion technique and at higher concentrations using isothermal titration calorimetry. In addition, the concentration of peptide monomers in solution was estimated by means of CD spectroscopy.

The apparent partition coefficient for neutral POPC membrane model systems decreased from $K_{app} = (1.2 \pm 0.2)\cdot10^4$ M^{-1} at $C_0 \sim 0.1$ μM to $K_{app} = (6.2 \pm 0.2)\cdot10^3$ M^{-1} at 10 μM. At the highest concentration only ~50% of H17 was in the monomeric form. At the lowest concentration measured H17 can be assumed to be monomeric.

The Hydrophobic and Electrostatic Contributions to Membrane Partitioning of H17—The binding isotherm of H17 measured for POPC/POPG (3/1) monolayers at 32 mN/m (Fig. 3C) was fitted by means of the Gouy-Chapman theory providing the hydrophobic and the electrostatic contributions of a peptide to membrane partitioning. The hydrophobic partition coefficient was determined as $K_p = 8.5\cdot10^3$ M^{-1} and is thus in close agreement with the apparent partition coefficient, $K_{app} = (1.2 \pm 0.2)\cdot10^4$ M^{-1}, determined for POPC monolayers. The total effective charge of H17 comprising the contribution from the N-terminal amino group and that of the five lysine residues was determined as $z_{eff} \cong +1.7$. This low charge of H17 when bound to lipid vesicles was experimentally corroborated by ζ-potential measurements.[3]

Considering the $pK_a = 10.53$ of free lysine in solution, this charge appears surprisingly small at first sight. A much lower charge than expected on the basis of the pK_a values of the individual amino acids in solution has, however, been observed for many other peptides with clusters of cationic residues. Examples are pentalysine (42), substance P (43), substance P antagonists (44), somatostatin (33), and melittin (45, 46). At least two factors are responsible for a charge reduction in these peptides. (i) Repulsive electrostatic interactions between clustered cationic amino acid residues lead to pK_a shifts (39), and (ii) the increase in peptide concentration close to the negatively charged membrane surfaces ($C_M > C_{eq}$) may induce peptide association which could also lead to pK_a shifts.

Among the peptides for which the hydrophobic and electrostatic contributions to binding have been determined by means of the Gouy-Chapman theory, melittin, a peptide from bee venom, shows the closest resemblance to H17, as shown in Table II.

The number of amino acid residues for H17 (melittin) are 22 (26), where 9 (13) residues are hydrophobic (indicated by bold letters in Table II) and 6 (6) carry a potential cationic charge, 5 (4) of which are at the C-terminal end. H17 carries in addition two negatively charged groups. The effective charge recognized

Downloaded from http://www.jbc.org/ at Universitaetsbibliothek Medizin on November 20, 2017

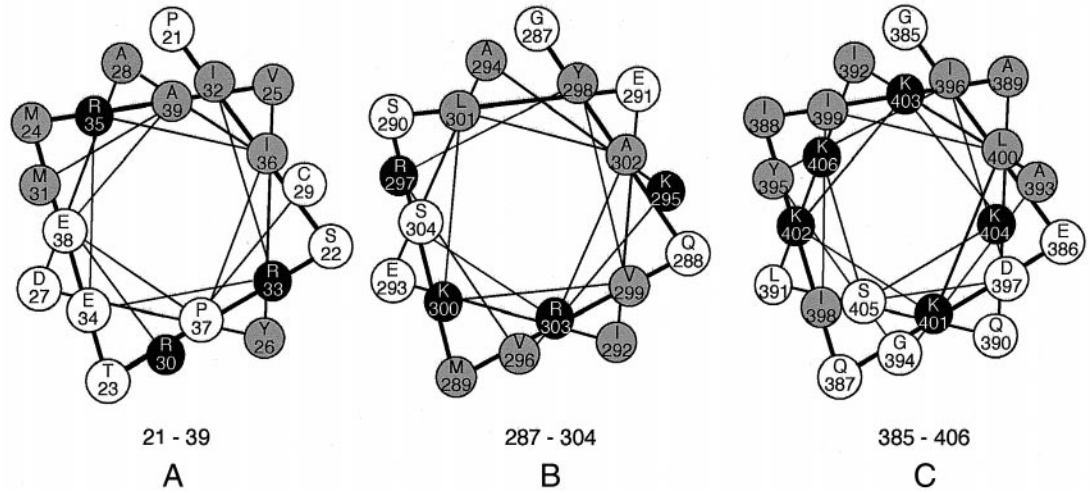

FIG. 6. **Helical wheel projections of the tree talin sequences 21–39 (S19), 287–304 (H18), and 385–406 (H17).** Hydrophobic residues (*gray*), hydrophilic residues (*white*), and cationic residues (*black*).

TABLE II
A comparison of amino acid sequences of H17 and melittin

	+− − ++++ +
H17	GEQ**IA**Q**LIA**GY**ID**I**IL**KKKKSK-$CONH_2$
	+ + ++++
Melittin	**GIGAVLKVL**TTG**LPALISWI**KRKRQQ-$CONH_2$

by the membrane was evaluated as $z_{eff} = +1.7$ for H17 and as $z_{eff} = +1.9$ for melittin (45). The hydrophobic free energy of H17 binding to POPC/POPG monolayers at 32 mN/m was determined as $\Delta G_0 = -7.8$ kcal/mol. The hydrophobic free energy of melittin binding to planar lipid bilayers was determined as $\Delta G_0 = -6.99$ kcal/mol (46) and that to SUVs as $\Delta G_0 = -8.83$ kcal/mol (45).

Membrane Partitioning of H17 Is Mainly Driven by Entropy—Membrane partitioning is thermodynamically characterized by the reaction enthalpy, ΔH_0, and the partition coefficient, K, or the free energy of reaction, ΔG_0 ($\Delta G_0 = \Delta H_0 - T\Delta S_0$) and can be determined using isothermal titration calorimetry. Partitioning of H17 ($C_0 = 2.5 \cdot 10^{-6}$ M) into negatively charged (and electrically neutral) SUVs yields a free energy, $\Delta G_0 = -8.2$ kcal/mol, (7.76 kcal/mol), an enthalpy, $\Delta H_0 = -2.4$ kcal/mol (−5.7 kcal/mol) and an entropy, $\Delta S_0 = +19.5$ cal/mol K (+6.8 cal/mol K). Membrane partitioning of H17 is thus enthalpy as well as entropy driven (positive $T\Delta S$ value). This is in contrast to the more hydrophilic peptides, somatostatin and analogs (33) and magainin and analogs (47, 48), which were shown to be enthalpy driven (exothermic reaction enthalpies and negative $T\Delta S$ values). An endothermic reaction enthalpy of +6 kcal/mol and a positive $T\Delta S$ value were, however, measured for the strongly hydrophobic cyclosporin A (35). In its thermodynamic behavior, H17 is thus in between the two types of peptides.

The Binding Energy of H17 Corresponds to That of Post-translationally Attached Membrane Anchors—To estimate whether the selected talin fragments provide enough binding energy to anchor talin at the membrane surface, we first compared the measured hydrophobic free energy of binding of H17 ($\Delta G_0 = -7.8$ kcal/mol) with that of myristoylated peptides and proteins. The hydrophobic free energy of binding of myristoylated peptides was determined as $\Delta G_0 = -7.9$ kcal/mol (49), in close agreement with that of myristoylated proteins such as hisactophilin I and II (22), and that of the α-subunit of transducin (50). The free energy of binding of farnesylated peptides was determined as $\Delta G_0 = -9.3$ kcal/mol (51) again in good agreement with that of the farnesylated $\beta\gamma$-subunit of transducin (50). The electrostatic contribution of H17 binding to negatively charged POPC/POPG (3/1) membranes was $\Delta G_0 = -1.6$ kcal/mol at pH 7.4 and became more negative with decreasing pH. At pH 7.4 the total free energy of binding (electrostatic plus hydrophobic contribution) thus amounts to $\Delta G_0 = -9.4$ kcal/mol for H17 and to $\Delta G_0 = -5.7$ kcal/mol for S19. The latter could act as an additional anchor.

In conclusion, we have shown that H17 with its highly specific combination of five isoleucines clustered in the hydrophobic face of a helix, and the five lysines clustered at the C terminus inserts into electrically neutral and negatively charged membranes. The insertion process is mainly entropy-driven. The hydrophobic free energy of binding, ΔG_0, of H17 is comparable to that of post-translationally attached membrane anchors. The additional electrostatic contribution to the free energy of binding arising from the cluster of lysine residues is pH-dependent. The present results thus suggest that sequence 385–406 (H17) may act as an intrinsic membrane anchor of talin. Sequence 21–39 (S19) could provide an additional (hydrophobic and electrostatic) contribution to talin anchorage at the lipid membrane.

REFERENCES

1. Burridge, K., and Connell, L. (1983) *J. Cell Biol.* **97,** 359–367
2. DePasquale, J. A., and Izzard, C. S. (1991) *J. Cell Biol.* **113,** 1351–1359
3. Burridge, K., and Mangeat, P. (1984) *Nature* **308,** 744–746
4. Horwitz, A., Duggan, K., Buck, C., Beckerle, M. C., and Burridge, K. (1986) *Nature* **320,** 531–533
5. Borowsky, M. L., and Hynes, R. O. (1998) *J. Cell Biol.* **143,** 429–442
6. Beckerle, M. C., Miller, D. E., Bertagnolli, M. E., and Locke, S. J. (1989) *J. Cell Biol.* **109,** 3333–3346
7. Knezevic, I., Leisner, T. M., and Lam, S. C. T. (1996) *J. Biol. Chem.* **271,** 16416–16421
8. Kreitmeier, M., Gerisch, G., Heizer, C., and Muller-Taubenberger, A. (1995) *J. Cell Biol.* **129,** 179–188
9. Moulder, G. L., Huang, M. M., Waterston, R. H., and Barstead, R. J. (1996) *Mol. Biol. Cell* **7,** 1181–1193
10. Kaufmann, S., Piekenbrock, T., Goldmann, W. H., Barmann, M., and Isenberg, G. (1991) *FEBS Lett.* **284,** 187–191
11. Kaufmann, S., Kas, J., Goldmann, W. H., Sackmann, E., and Isenberg, G. (1992) *FEBS Lett.* **314,** 203–205
12. Niewöhner, J., Weber, I., Maniak, M., Muller-Taubenberger, A., and Gerisch, G. (1997) *J. Cell Biol.* **138,** 349–361
13. Albiges-Rizo, C., Frachet, P., and Block, M. R. (1995) *J. Cell Sci.* **108,** 3317–3329
14. Nuckolls, G. H., Romer, L. H., and Burridge, K. (1992) *J. Cell Sci.* **102,** 753–762
15. Hemmings, L., Rees, D. J., Ohanian, V., Bolton, S. J., Gilmore, A. P., Patel, B., Priddle, H., Trevithick, J. E., Hynes, R. O., and Critchley, D. R. (1996) *J. Cell Sci.* **109,** 2715–2726
16. McCann, R. O., and Craig, S. W. (1997) *Proc. Natl. Acad. Sci. U. S. A.* **94,** 5679–5684
17. Goldmann, W. H., Bremer, A., Haner, M., Aebi, U., and Isenberg, G. (1994) *J. Struct. Biol.* **112,** 3–10
18. Goldmann, W. H., Guttenberg, Z., Kaufmann, S., Hess, D., Ezzell, R. M., and Isenberg, G. (1997) *Eur. J. Biochem.* **250,** 447–450
19. Goldmann, W. H., Hess, D., and Isenberg, G. (1999) *Eur. J. Biochem.* **260,**

Downloaded from http://www.jbc.org/ at Universitaetsbibliothek Medizin on November 20, 2017

439–445
20. Niggli, V., Kaufmann, S., Goldmann, W. H., Weber, T., and Isenberg, G. (1994) *Eur. J. Biochem.* **224,** 951–957
21. Goldmann, W. H., Senger, R., Kaufmann, S., and Isenberg, G. (1995) *FEBS Lett.* **368,** 516–518
22. Hanakam, F., Gerisch, G., Lotz, S., Alt, T., and Seelig, A. (1996) *Biochemistry* **35,** 11036–11044
23. Tempel, M., Goldmann, W. H., Isenberg, G., and Sackmann, E. (1995) *Biophys. J.* **69,** 228–241
24. Johnson, R. P., Niggli, V., Durrer, P., and Craig, S. W. (1998) *Biochemistry* **37,** 10211–10222
25. Isenberg, G., and Goldmann, W. H. (1998) *FEBS Lett.* **426,** 165–170
26. Seelig, A. (1987) *Biochim. Biophys. Acta* **899,** 196–204
27. Rees, D. J., Ades, S. E., Singer, S. J., and Hynes, R. O. (1990) *Nature* **347,** 685–689
28. Yang, J. T., Wu, C. S., and Martinez, H. M. (1986) *Methods Enzymol.* **130,** 208–269
29. Greenfield, N., and Fasman, G. D. (1969) *Biochemistry* **8,** 4108–4116
30. Chen, Y. H., Yang, J. T., and Chau, K. H. (1974) *Biochemistry* **13,** 3350–3359
31. Fromherz, P. (1975) *Rev. Sci. Instrum.* **46,** 1380
32. Boguslavsky, V., Rebecchi, M., Morris, A. J., Jhon, D. Y., Rhee, S. G., and McLaughlin, S. (1994) *Biochemistry* **33,** 3032–3037
33. Seelig, J., Nebel, S., Ganz, P., and Bruns, C. (1993) *Biochemistry* **32,** 9714–9721
34. Wiseman, T., Williston, S., Brandts, J. F., and Lin, L. N. (1989) *Anal. Biochem.* **179,** 131–137
35. Seelig, J. (1997) *Biochim. Biophys. Acta* **1331,** 103–116
36. Terzi, E., Hölzemann, G., and Seelig, J. (1994) *Biochemistry* **33,** 1345–1350
37. Duysens, L. N. M. (1956) *Biochim. Biophys. Acta* **19,** 1–12
38. Seelig, A., Alt, T., Kürz, L., and Mutter, M. (1993) in *Peptides 1992* (Schneider, C. H., and Eberle, A. N., eds) pp. 113–114, ESCOM Science Publishers B.V., ESCOM, Leiden, Netherlands
39. Seelig, A. (1990) *Biochim. Biophys. Acta* **1030,** 111–118
40. Schiffer, M., and Edmundson, A. B. (1967) *Biophys. J.* **7,** 121–135
41. Doebler, R., Basaran, N., Goldston, H., and Holloway, P. W. (1999) *Biophys. J.* **76,** 928–936
42. Montich, G., Scarlata, S., McLaughlin, S., Lehrmann, R., and Seelig, J. (1993) *Biochim. Biophys. Acta* **1146,** 17–24
43. Seelig, A., and Macdonald, P. M. (1989) *Biochemistry* **28,** 2490–2496
44. Seelig, A. (1992) *Biochemistry* **31,** 2897–2904
45. Beschiaschvili, G., and Seelig, J. (1990) *Biochemistry* **29,** 52–58
46. Kuchinka, E., and Seelig, J. (1989) *Biochemistry* **28,** 4216–4221
47. Wieprecht, T., and Seelig, J. (2000) *Biophys. J.* **78,** 959
48. Wieprecht, T., Apostolov, O., Beyermann, M., and Seelig, J. (2000) *Biochemistry* **39,** 442–452
49. Peitzsch, R. M., and McLaughlin, S. (1993) *Biochemistry* **32,** 10436–10443
50. Seitz, H. R., Heck, M., Hofmann, K. P., Alt, T., Pellaud, J., and Seelig, A. (1999) *Biochemistry* **38,** 7950–7960
51. Silvius, J. R., and Lheureux, F. (1994) *Biochemistry* **33,** 3014–3022
52. Evans, R. W., Williams, M. A., and Tinoco, J. (1987) *Biochem. J.* **245,** 455–462

Downloaded from http://www.jbc.org/ at Universitaetsbibliothek Medizin on November 20, 2017

Phospholipid Binding of Synthetic Talin Peptides Provides Evidence for an Intrinsic Membrane Anchor of Talin

Anna Seelig, Xiaochun Li Blatter, Adrian Frentzel and Gerhard Isenberg

J. Biol. Chem. 2000, 275:17954-17961.
doi: 10.1074/jbc.M002264200 originally published online March 27, 2000

Access the most updated version of this article at doi: 10.1074/jbc.M002264200

Alerts:
- When this article is cited
- When a correction for this article is posted

Click here to choose from all of JBC's e-mail alerts

This article cites 51 references, 13 of which can be accessed free at
http://www.jbc.org/content/275/24/17954.full.html#ref-list-1

Downloaded from http://www.jbc.org/ at Universitaetsbibliothek Medizin on November 20, 2017